

BCSJ Award Article

Chemistry of Anthracene–Acetylene Oligomers XV. Synthesis, Structures, and Dynamic Behavior of Chiral Anthrylene–Ethynylene Cyclic Tetramers and Related Derivatives and Resolution of Enantiomers[1]

Takeharu Ishikawa,[1] Toshiaki Shimasaki,[3] Haruo Akashi,[2] Tetsuo Iwanaga,[1] Shinji Toyota,*[1] and Mikio Yamasaki[4]

[1]Department of Chemistry, Faculty of Science, Okayama University of Science, 1-1 Ridaicho, Kita-ku, Okayama 700-0005

[2]Research Institute of Natural Sciences, Okayama University of Science, 1-1 Ridaicho, Kita-ku, Okayama 700-0005

[3]Department of Chemistry, Faculty of Science, Kyushu University, 6-10-1 Hakozaki, Higashi-ku, Fukuoka 812-8581

[4]Rigaku Corporation, 3-9-12 Matsubaracho, Akishima, Tokyo 196-8666

Received October 8, 2009; E-mail: stoyo@chem.ous.ac.jp

A cyclic arylene–ethynylene tetramer with a 1,5-anthrylene unit and a cramp moiety consisting of three anthrylene units and its derivatives with a 1,4-phenylene, 1,5-naphthylene, or 2,6-di-*t*-butyl-1,5-naphthylene unit were synthesized by macrocyclization with Sonogashira coupling. Except for the 1,4-phenylene compound, these cyclic compounds take the chiral C_2 structure with parallel orientation of the two arylene units, as revealed by X-ray analysis and DFT calculation at the M05/3-21G level. The enantiomers of 1,5-anthrylene and 2,6-di-*t*-butyl-1,5-naphthylene compounds were resolved by chiral HPLC and their rotational barriers were determined to be 114 and $>146\,kJ\,mol^{-1}$, respectively, by classical kinetics. These high barriers are in contrast to the facile racemization or topomerization in the other compounds. These kinetic data of the rotation of arylene units about the acetylene axes are discussed in terms of steric hindrance based on molecular structures. The electronic spectra of the cyclic compounds and the chiroptical properties of the resolved samples were also measured.

Arylene–ethynylene oligomers and polymers are attractive molecules in the study of the structures and properties of π-conjugated compounds, and their recent applications to molecular machines, functional materials, and supramolecules are noteworthy.[2] The versatility of the molecular design resulting from the variations in arylene units, their numbers, and the connection sites allows for the construction of a large number of oligomers with multiple structures and flexibility, which contribute significantly to their properties. The rotation of arylene units about ethynylene linkers occasionally leads to a key motion in the molecular design. For example, Garcia-Garibay and co-workers intelligently utilized the rotation of 1,4-phenylene moieties to realize molecular gyroscopes in the solid state.[3] Round wheel moieties such as C_{60} are connected to the body by an acetylenic axle in various models of nano-cars designed by Tour's group and other molecular vehicles.[4] In those structures, the acetylene linkers are regarded as axles connecting two moieties with virtually free rotation. Actually, the rotational barriers in diphenylethyne, the simplest building unit, and related simple alkynes are $3\,kJ\,mol^{-1}$ or lower.[5] The barriers can be enhanced by introducing sterically demanding substituents to the fundamental structure. For example, barrier heights were studied by dynamic NMR for diphenylethyne derivatives with four phenyl groups ($51\,kJ\,mol^{-1}$)[6] or four (trialkylsilyl)ethynyl groups ($78\,kJ\,mol^{-1}$)[7] at all the *ortho*-positions. The rotation is also restricted in di(9-anthryl)ethyne and di(9-triptycyl)ethyne derivatives with bulky substituents on the NMR time scale.[8] For cyclic systems, restricted rotation is utilized in the design of turnstile molecules by Bedard and Moore.[9] The rotational barrier of a phenylene spindle moiety surrounded by a rigid macrocycle is enhanced by a bulky substituent on the phenylene group ($>86\,kJ\,mol^{-1}$).

We have extensively utilized 1,8-anthrylene units for the construction of new types of arylene–ethynylene π-conjugated oligomers, such as cyclic tetramer **1**,[10,11] trimer **2**,[12] dimer **3**,[13] and their derivatives with substituents or longer linkers (Figure 1). Some cyclic tetramers undergo skeletal dynamic processes via rotation about the acetylene linkers as revealed by dynamic NMR study. Therefore, we designed new cyclic structures **4** with a view to isolating stereoisomers generated by restricted rotation about the acetylene linkers (Figure 2).

Published on the web February 26, 2010; doi:10.1246/bcsj.20090270

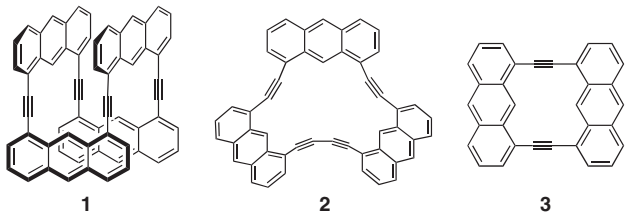

Figure 1. Frameworks of various 1,8-anthrylene–ethynylene cyclic oligomers.

Compound **4d** consists of four anthracene units connected at various positions by acetylene linkers, where a crank 1,5-anthrylene unit [(1,5)-A; for abbreviations, see Figure 2] is incorporated.[1] This molecule is expected to take a chiral structure to relieve the steric interactions between (1,5)-A and (9,10)-A, and a pedaling motion of the crank moiety accompanied by the rotation about the acetylene axes results in enantiomerization. We also introduced crank 1,5-naphthylene units in **4b**[1] and **4c** and a linear 1,4-phenylene unit in **4a** in place of (1,5)-A in **4d** to examine the effects of the length and bulkiness of the crank moieties as well as the mode of connection. These compounds **4** are considered to be members of cyclophynes, cyclic arylene oligomers with ethynylene or longer acetylene linkers.[14] Although a large number of enantiopure cyclophynes have been reported, most of them contain chiral arylene units such as binaphthyls and helicenes.[15] Therefore, except for **4a**, our target compounds are notable because they have only the stereogenic axes along the acetylene linkers. The enantiomers of **4c** and **4d** were successfully resolved at room temperature by chiral HPLC because of the highly restricted rotation of the crank moiety about the acetylene axes. We report herein the synthesis, structures, and properties of these cyclic tetramers as novel π-conjugated compounds. Chiroptical properties and ease of racemization of the enantiomers resolved by chiral HPLC are also described.

Results and Discussion

Synthesis. The target compounds were synthesized according to the route shown in Scheme 1. Cramp moiety **7** was prepared by Sonogashira coupling of **5**[10b] and **6**[16] in 2:1 ratio, where a butyl group was introduced to each (1,8)-A moiety to increase solubility. Compound **7** was treated with tetrabutylammonium fluoride (TBAF) in CH_2Cl_2 to form a mixture of desilylated products **8** and **9**, and the former was separated by chromatography. Compound **8** was coupled with an excess of diiodoarenes **10** to give corresponding tetramers **11** with a small amount of heptamers **12**. Tetrameric precursors **11** were desilylated with TBAF and the formed terminal alkynes were subjected to Sonogashira coupling without purification. The desired cyclic products were obtained by chromatography and recrystallization as orange crystals in 72% yield for **4a** and in ca. 30% yield for **4b**–**4d**. The molecular ion peaks of these products were observed by FAB mass spectroscopy. The ^{1}H NMR spectra of the tetramers became simple upon cyclization, reflecting the higher symmetry. The details of the signal pattern will be discussed later.

Molecular Structures. X-ray analyses were carried out for **4a**, enantiopure **4c**, and racemic **4d**. ORTEP drawings are shown in Figure 3. Arene units are nearly planar in each structure except one of the (1,8)-A units in **4c**, in which some torsion angles within the anthracene carbons are off by 5–6° from 0 or 180°. The acetylene linkers are nearly linear as indicated by bond angles at sp carbons (175–180°), while there are small bending deformations at two sp carbons in **4a**, as indicated in Figure 3. The structure of the cyclic framework is characterized by the dihedral angles between the arene units. In the structure of **4a**, (1,8)-A planes are nearly perpendicular to the (9,10)-A plane, and (1,4)-P plane is nearly coplanar with the (1,8)-A planes. As a result, the (1,4)-P moiety is perpendicular to the (9,10)-A plane, where the distance between the two inner phenylene hydrogen atoms and the (9,10)-A plane is ca. 2.8 Å. This distance is nearly equal to the

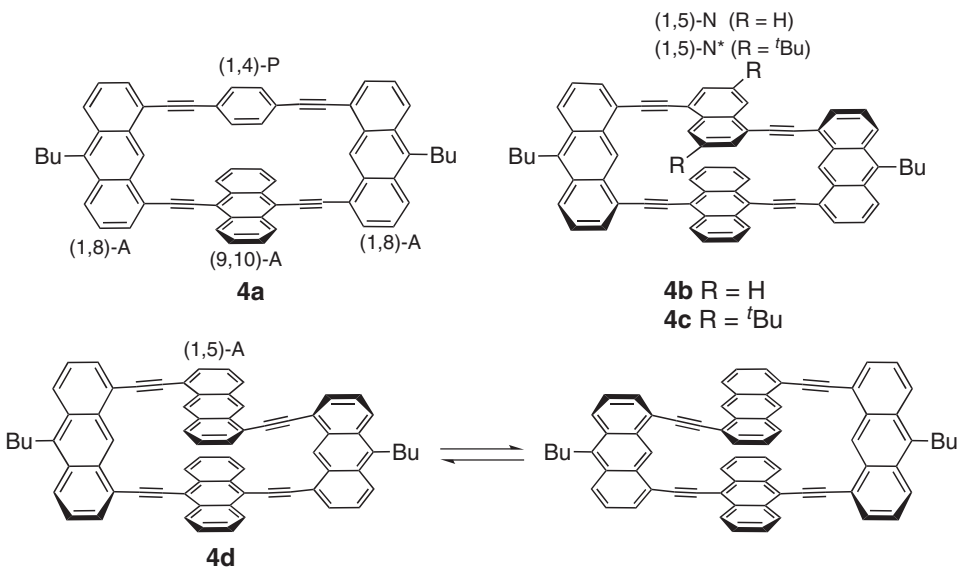

Figure 2. Structures of target cyclic tetramers **4** with the abbreviation of each arylene unit.

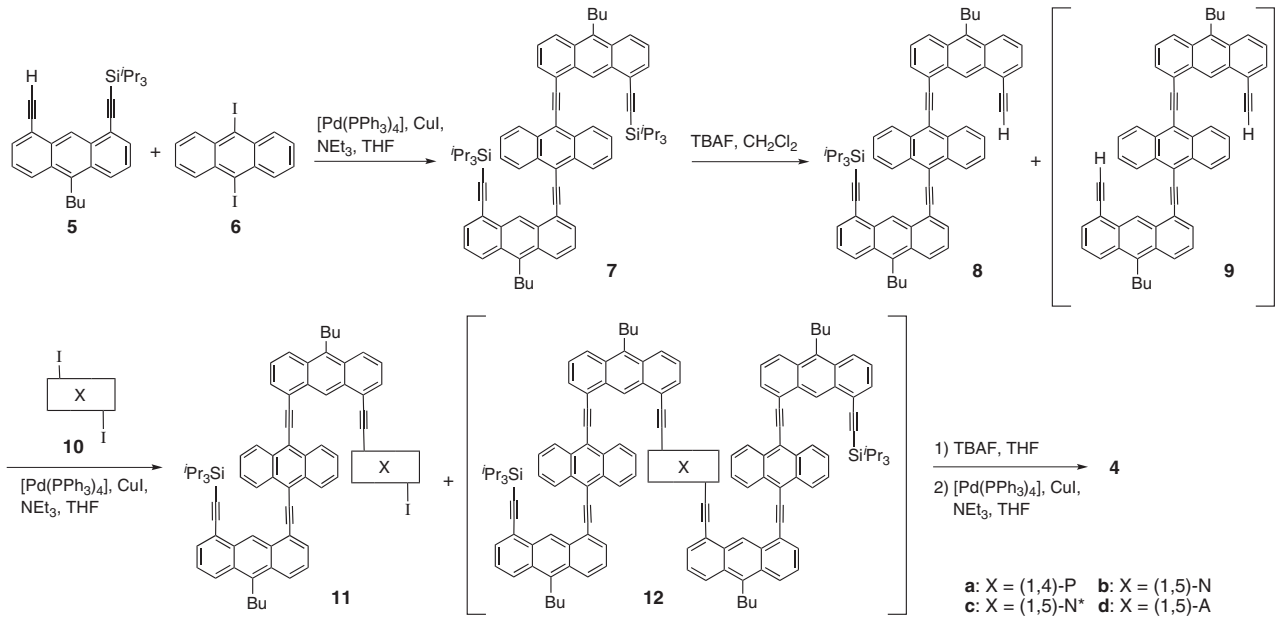

Scheme 1. Synthesis of cyclic tetramers **4**.

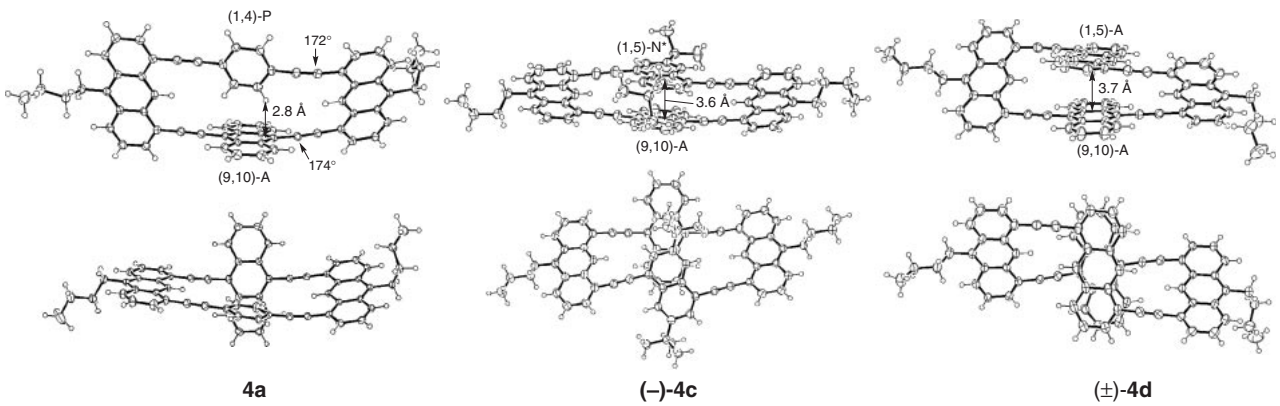

Figure 3. Two views of X-ray structures of **4a**, (−)-**4c**, and (±)-**4d** with thermal ellipsoids at 50% probability. Solvent molecules are omitted for clarity for (±)-**4d**. Selected bond angles at sp carbons (<175°) are indicated. Absolute stereochemistry is arbitrary.

sum of the van der Waals radii of H (1.2 Å) and Csp^2 (1.7 Å), suggesting transannular C–H···π interactions.[17] The structure of **4d** is approximately C_2 symmetric, where the dihedral angles between (1,8)-A and (9,10)-A and those between (1,8)-A and (1,5)-A are all ca. +40 or −40°. The two anthracenes, (9,10)-A and (1,5)-A, are almost parallel (dihedral angle 4.6°) and completely overlap each other, separated by a distance of 3.67 Å. This distance is comparable to the distance required for π···π interactions between aromatic moieties. A similar parallel orientation is also seen in **4c**, where the distance between the two arylene planes is ca. 3.6 Å, while (1,5)-N* moiety apparently slides to the flanking side of (9,10)-A with a small tilt (dihedral angle 12°). Accordingly, one ^{t}Bu group is located above (9,10)-A and the other is away from it.

To obtain further structural information, we carried out DFT calculations for butyl-free compounds **4′**. The structures of **4d′** were preliminarily optimized at various levels because the choice of density functionals and basis sets plays an important role in reproducing the experimental structures. Although the calculation at the B3LYP/6-31G level gave a C_2 symmetric structure with parallel orientation of (1,5)-A and (9,10)-A planes, the interlayer distance (4.42 Å) is much longer than that observed. This discrepancy is attributed to the underestimation of attractive interactions between aromatic moieties. To overcome this limitation, a new series of widely applicable functionals called M05 were developed by Truhlar's group.[18] The interlayer distances calculated by the M05 and M05-2X functionals were 3.67 and 3.13 Å, respectively, with the 3-21G basis set, and the former was in good agreement with the experimental. Therefore, we carried out the calculations of **4′** at the M05/3-21G level (Figure 4), which was also adopted for the calculations of 1,8-anthrylene cyclic oligomers.[11] The experimental structure of **4c** was approximately reproduced by the calculation of **4c′**, including the orientation and the distance of nearly parallel arene moieties (**4c′**-C_1 in Figure 4), although another minimum structure of approximately C_2 symmetry (**4c′**-C_2) was also obtained at an energy level less stable by only 1.5 kJ mol^{-1}. The optimized structure of **4b′** is C_2 symmetric with an interlayer distance of 3.6 Å, which is comparable to that in **4d′**. On the other hand, the orientation of (1,4)-P moiety in

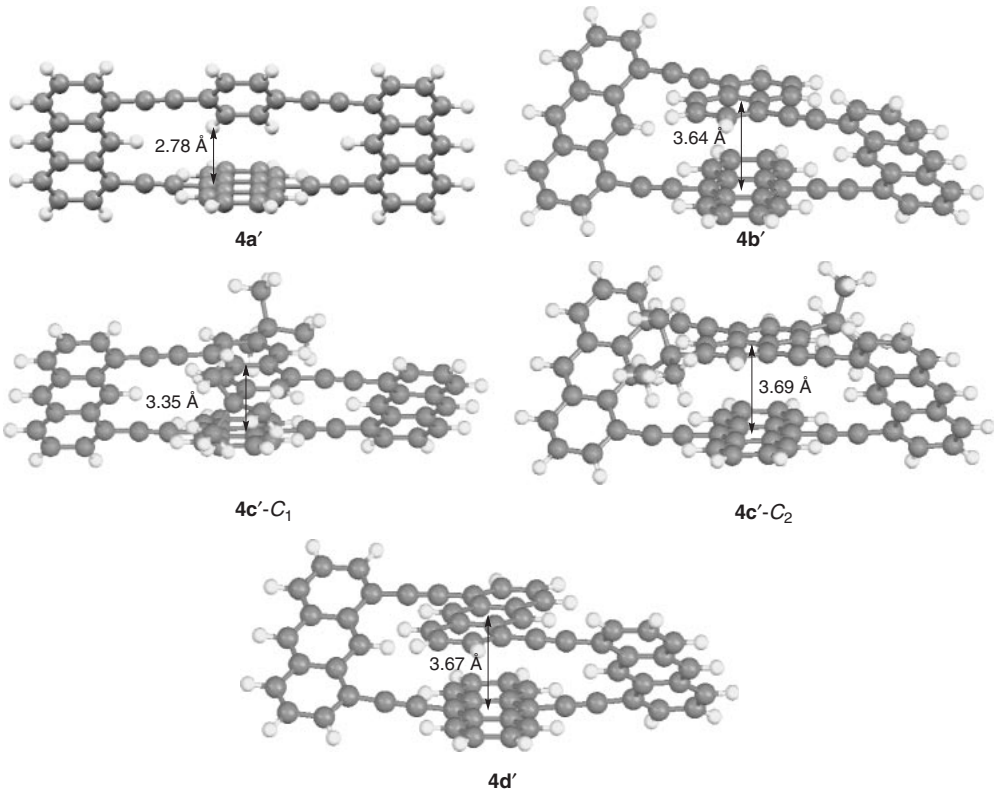

Figure 4. Optimized structures of **4′** without butyl groups at the M05/3-21G level. Important C–H···π (**4a′**) or π···π (**4b′**–**4d′**) distances are given.

4a′ is very sensitive to the calculation method because the rotation about the linear axes takes place easily. Nevertheless, the calculation at the M05/3-21G level well reproduced the X-ray structure with the C–H···π contacts between (1,4)-P and (9,10)-A (calcd 2.78 Å). The two arene moieties in **4a′** are separated too far in the structure optimized by B3LYP due to underestimation of the nonbonding interactions, and nearly parallel in the structure optimized by M05-2X due to overestimation of the π···π interactions.

Electronic Spectra. The UV–vis and fluorescence spectra of the cyclic tetramers and their acyclic precursors were measured in chloroform. The data are listed in Table 1. Absorption bands in the p-band region were observed in the range of 380–540 nm as broad peaks (Figure 5). The peaks or shoulders at the longest wavelength appeared at ca. 480 nm for all cyclic tetramers **4** as well as precursors **11**. The effect of cyclization is rather small as also observed in the system of 1,8-anthrylene cyclic tetramers.[11] The wavelength of **4d** with four anthrylene units is significantly longer than that of cyclic tetramer **1** bearing two butyl groups (448 nm).[10] This difference is attributed to the presence of 9,10-diethynylanthracene chromophores, which results in a large bathochromic effect relative to ethynyl-substituted anthracenes at the other positions.[19] For example, the absorption bands at the longest wavelength were observed at 413, 414, and 440 nm for 1,8-, 1,5-, and 9,10-bis[(trialkylsilyl)ethynyl]anthracenes, respectively.[10b,20] The above data also mean that the effects of the incorporated arene units on the wavelength are insignificant. This result was further explored by MO analysis of the DFT calculations. The intense absorptions at the longest wavelength were mostly attributed to transition from HOMO to LUMO in **4a**–**4d**, where the orbital lobes were mainly distributed on the 9,10-diethynylanthracene and the attaching (1,8)-A moieties (Supporting Information). Namely, the common chromophore plays a dominant role in the HOMO–LUMO transition, and the transannular interactions between the facing arene units are not so large as to influence the absorption bands in this region. In contrast, remarkable interactions were observed between anthracene chromophores in [2.2]anthracenophanes leading to large bathochromic and hypochromic effects.[21] The X-ray

Table 1. UV–Vis and Fluorescence Spectral Data of Cyclic Oligomers **4** with Their Acyclic Precursors **11** in Chloroform

	UV	FL[b)]			Stokes shift /nm
	λ_{max}/nm (ε)[a)]	λ_{max} /nm	Φ_f[c)]	τ_f /ns[d)]	
4a	446 (23600), 481 (15300, sh)	525	0.67	3.2	44
4b	482 (25900)	525	0.69	3.1	43
4c	489 (23300)	525	0.74	3.3	36
4d	453 (36300), 477 (30600)	547	0.54	6.8	70
11a	454 (33000), 474 (31000, sh)	524	0.52	2.2	70
11b	476 (34000)	525	0.31	1.3	49
11c	479 (32000)	525	0.41	1.8	46
11d	448 (35000), 483 (34000)	529	0.16	1.3	46

a) Wavelengths and molar extinction coefficients of main maximum absorptions and shoulders in the p-band region. b) Excited at 393 nm. c) Absolute fluorescence quantum yield. d) Fluorescence lifetime.

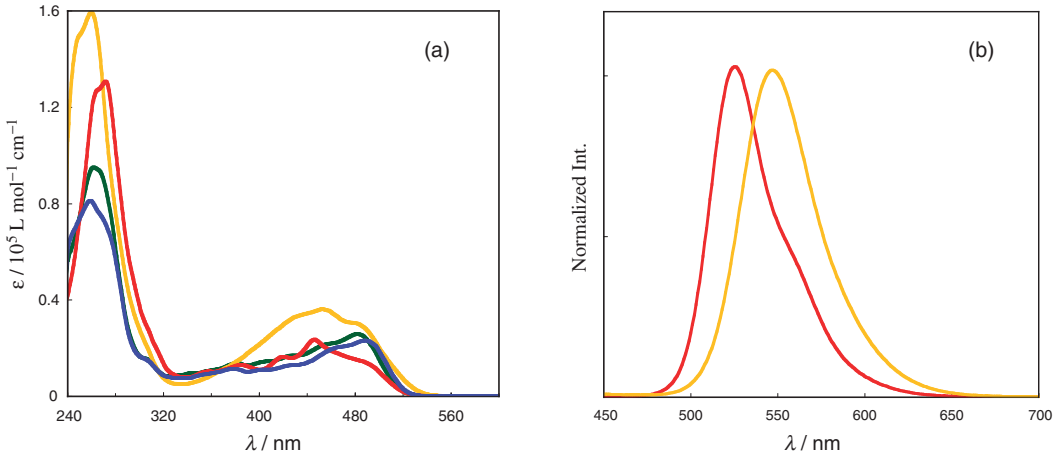

Figure 5. UV–vis (a) and fluorescence (b) spectra of **4a** (red), **4b** (green), **4c** (blue), and **4d** (yellow) in $CHCl_3$. Fluorescence spectra of **4b** and **4c** are not shown as they are almost superimposable with that of **4a**.

analysis of these derivatives revealed that the two anthracene units were tightly connected with two ethano bridges, where the interlayer distances were ca. 3.3 Å or even shorter. In the observed and calculated structures of **4**, the interlayer distances are larger than those in the anthracenophanes and the arene units still have freedom of motion. We consider that this structural situation is a reason for the very small substituent effects on the absorption spectra of compounds **4**.

The cyclic tetramers showed intense emission bands peaking at 525 nm for **4a**–**4c** and 547 nm for **4d**. As a result, the Stokes shift of **4d**, 70 nm, is larger than those of the other cyclic compounds. The absolute fluorescence quantum yields Φ_f of **4** are in the range of 0.54–0.74, being small compared with that of 9,10-bis(phenylethynyl)anthracene (0.89).[22] Conventional measurements showed that the emission of compounds **4** consisted of one component in contrast to cyclic tetramer **1** that exhibited the emission of two components at 2.4 and 14.7 ns due to monomer and excimer-type emissions, respectively.[10] The emission of **4d** features a long lifetime (6.8 ns) and a large Stokes shift (70 nm) compared with that of the other cyclic oligomers. The lifetime of **4d** is comparable to those of anthracenophanes, which were regarded as a model of excimer formation.[23] The large Stokes shift was observed in cyclophanes with effective intramolecular aromatic stacking.[24] Further careful measurements revealed that only **4d** gave an extra transient emission in the early stage (<0.5 ns) at 535 nm, which was slightly blue-shifted relative to the overall emission peak (Supporting Information). This observation means that a structural change takes place in the excited state in the sub-ns order to give a more stable excited state. These are evidence supporting the excimer-like character of the emission of **4d**.

Dynamic Behavior. The variable temperature (VT) ^{1}H NMR spectra of compounds **4** were measured to observe their dynamic behavior (Supporting Information). A possible dynamic process in **4a** is illustrated in Scheme 2a: rotation of (1,4)-P by 180° about the acetylene axes. If this rotation were frozen on the NMR time scale, the phenylene protons should give two peaks due to the outer and inner protons, H_A and H_B. The signals for these protons that were located in the shielding region of (9,10)-A were observed at δ 6.77 as a singlet at room temperature, and this signal pattern was virtually retained at −90 °C in CD_2Cl_2 even though all the signals became broad at low temperature. This broadening is attributed to the restricted rotation of butyl groups[10b,25] and the poor resolution, rather than the restricted rotation of (1,4)-P moiety.

Two dynamic processes of **4d** are shown in Schemes 2b and 2c as a representative of C_2 symmetric cyclic oligomers **4b**–**4d**. The rotation of (1,5)-A and (9,10)-A moieties by 180° leads to enantiomerization and topomerization, respectively. The signal pattern of (9,10)-A protons is affected by the rates of the two processes. If both processes are sufficiently slow on the NMR time scale, the probe signals should appear as an ABCD system. Actually, such signals were observed for **4c** and **4d** at room temperature (Figure 6), and this signal pattern was retained at 120 °C in 1,1,2,2-tetrachloroethane-d_2 (TCE-d_2). Under the same conditions, irradiation of the doublet at δ 8.56 (H_A or H_D) decreased the intensity of the other doublet at δ 8.16 for **4d**. This spin saturation transfer was quantitatively analyzed to give the rate of site exchange $k = 0.27\,s^{-1}$ at 120 °C corresponding to $\Delta G^{\neq}_{393} = 102 \pm 2\,kJ\,mol^{-1}$.[26] A similar measurement was also carried out for **4c**, but no transfer was observed even at 140 °C. This means that the exchange should take place much more slowly than the T_1 time scale, and the lower limit of the exchange barrier is estimated to be 108 kJ mol^{-1}. In contrast, the signals due to (9,10)-A in **4b** were observed as two multiplets (an AA′BB′ system) at room temperature and even at −90 °C in CD_2Cl_2. This observation indicates facile site exchange between H_A and H_D (or H_B and H_C) via either of the two processes to give the averaged signals. The rotation of (1,5)-N and/or (9,10)-A takes place much more rapidly than the NMR time scale.

Another possible dynamic process in **4c** is illustrated in Scheme 2d: the sliding of (1,5)-N* from one flanking side of (9,10)-A to the other side without tumbling, which results in site exchange between the two ^{t}Bu groups. The signal due to the ^{t}Bu groups was observed as a singlet at −60 °C although all signals underwent broadening at lower temperature due to the restricted rotation of the butyl groups. This observation is consistent with the DFT calculations mentioned above: the two structures of C_1 and C_2 symmetry have comparable energy, where the latter is regarded as a model of the transition state of the sliding motion. Therefore, the structure of **4c** is thought to

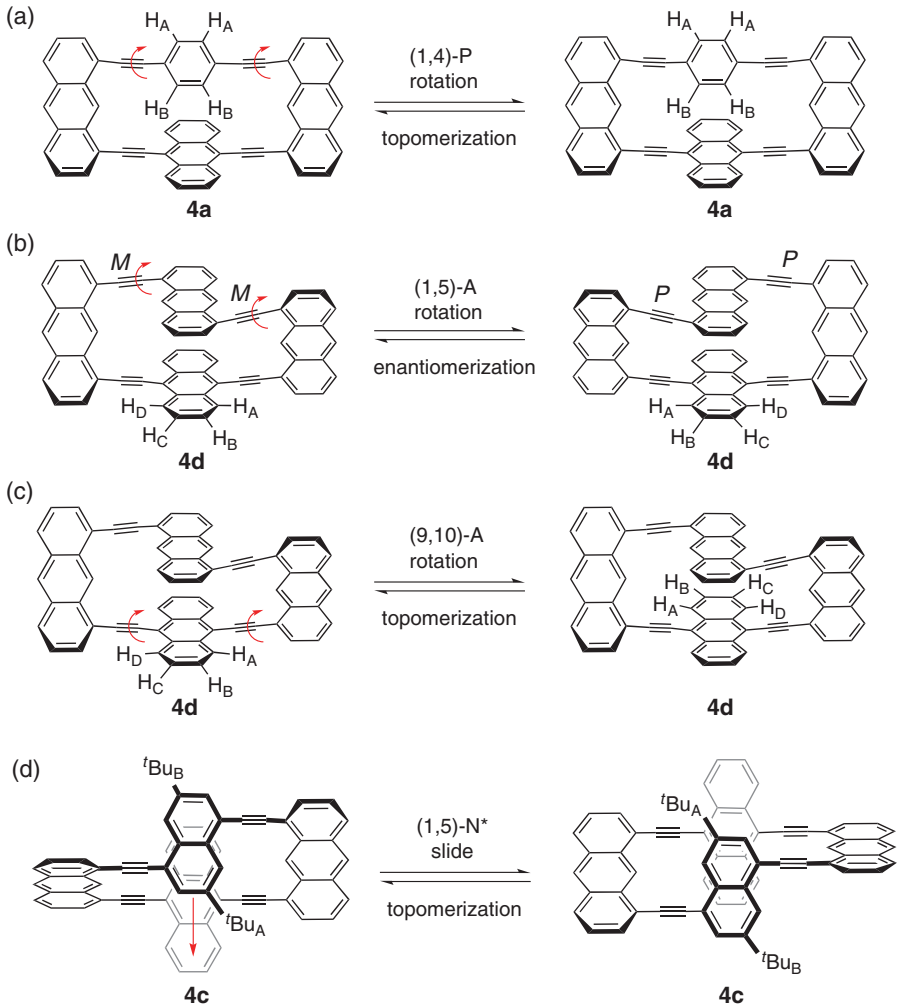

Scheme 2. Possible site exchanges in cyclic oligomers **4**. (a) Rotation of (1,4)-P in **4a**. (b) Rotation of (1,5)-A in **4d**. (c) Rotation of (9,10)-A in **4d**. (d) Sliding of (1,5)-N* in **4c**. Butyl groups are omitted for simplicity.

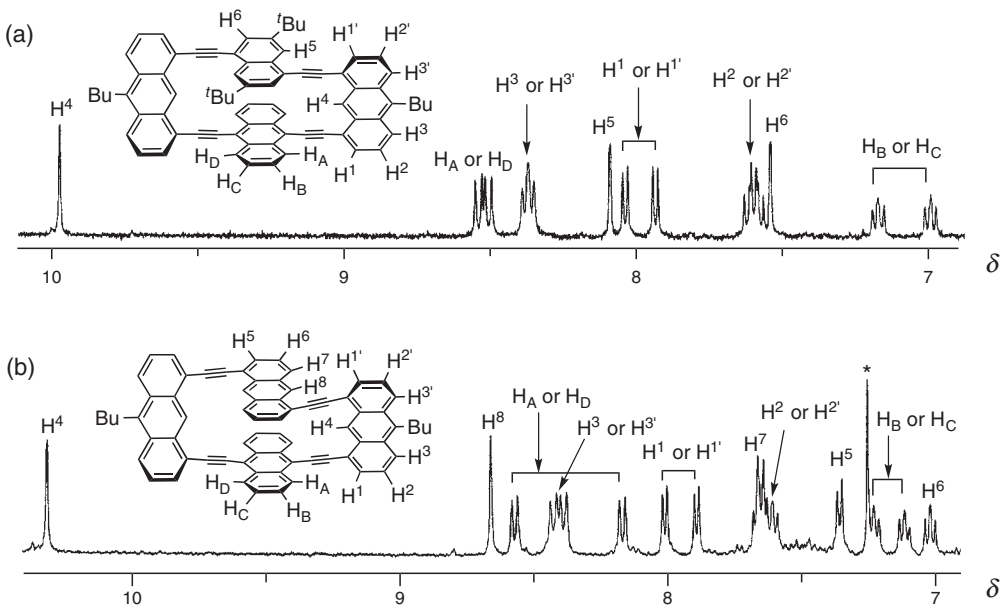

Figure 6. ^{1}H NMR spectra of **4c** and **4d** in the aromatic region in TCE-d_2. Signals were assigned with the aid of COSY and NOE measurements. * A signal due to chloroform.

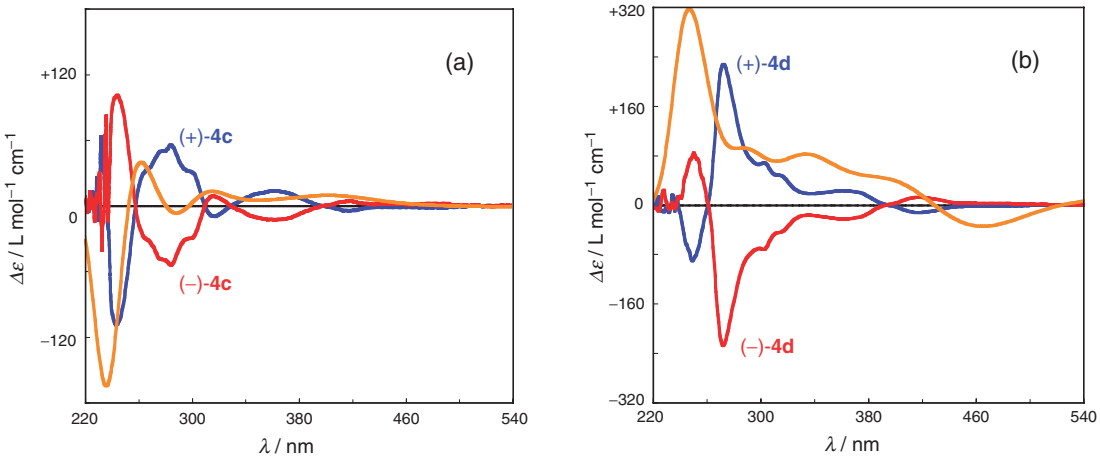

Figure 7. CD spectra of enantiopure **4c** (a) and **4d** (b) in $CHCl_3$ [blue: (+)-isomer, red: (−)-isomer] and calculated spectra for their *M*,*M* isomers by TDDFT at the B3LYP/3-21G//M05/3-21G level (orange).

be C_2 symmetric on the NMR time scale because of the facile sliding motion in solution.

Enantiomeric Resolution. The VT NMR measurements suggested the possibility of resolution of **4c** and **4d** at room temperature. Racemic samples of these compounds were subjected to chiral HPLC under various conditions, and the enantiomers were finally resolved with a Daicel Chiralpak IA column that featured the use of a broad range of eluent systems, under standard conditions.[27,28] The enantiomers of **4d** were separated by this column surprisingly well for hydrocarbon samples, and the retention times were 27.2 and 52.4 min (separation factor α 2.96) with hexane:2-propanol:chloroform (50:1:1) as eluent. The specific rotations of the first and second fractions were $[\alpha]_D^{22}$ +800 and −830, respectively. Compound **4c** was partially resolved at the retention times of 33.2 and 34.4 min with hexane:2-butanol (100:1) as eluent, and enantiopure samples were obtained by repeated separations. The specific rotations of the first and second fractions were $[\alpha]_D^{22}$ +800 and −850, respectively. The CD spectra of the resolved enantiomers are compiled in Figure 7, where the enantiomers gave mirror image bands of each other. The spectrum of the easily eluted sample, (+)-**4d**, showed a trough at 249 nm and an intense peak at 272 nm in the β-band region in addition to a weak trough at 418 nm in the p-band region. A sample of (+)-**4c** gave a trough at 243 nm and overlapping peaks at 260–300 nm. This spectral pattern is partly similar to that of (+)-**4d**, although these data do not always ensure the stereochemical relationship between the two (+)-isomers.

From a stereochemical aspect, compounds **4b**–**4d** are considered to be chiral with respect to a plane defined by (1,5)-arylene moieties. However, it is not straightforward to define the pilot atom and the adjacent three atoms in the plane. Therefore, we prefer to designate the stereochemistry in terms of the helical arrangement of (1,8)-A and (1,5)-A moieties along the acetylene axes. For example, the two axes have *M* helicity in the structure of **4d** shown on the left in Scheme 2b, designated as *M*,*M* or just *M*.[29] The chiroptical properties of the enantiomers of **4c** and **4d** should depend on the orientation of aromatic chromophores. Although we carefully analyzed the X-ray data of (−)-**4c**, the anomalous dispersion effect was found to be negligible as indicated by the Flack parameter. Although these molecules contain a large number of atoms, 120 or more, we managed to calculate the CD spectra by the TDDFT method.[30] The theoretical spectra calculated at the B3LYP/3-21G level with the structures in Figure 4 are compiled in Figure 7. When we consider the systematic shift of this calculation method, namely, the 20–40 nm red shift in the p-band region,[31] the first negative band at 417 nm and the following continuous peaks at 300–380 nm for the (+)-isomer are reproduced by the calculation for the *M*,*M* isomer. The blue shift of the peak in the short wavelength region is attributed to computational limitation, a limit in the number of excited states, as well as the systematic shift. Although there are some discrepancies, it seems to be reasonable to assign the (+)-isomer to *M*,*M* and the (−)-isomer to *P*,*P*. The calculation and comparison of the CD spectra of **4c** are more complicated because of the molecular size and the ease of conformational changes involving the sliding motion of (1,5)-N* and the rotation of methyl groups. The calculated curve looks similar to the observed spectra of the (+)-isomer rather than that of the (−)-isomer; one example is the intense trough at 240 nm. Further experiments or calculations are needed to obtain conclusive evidence of the absolute chemistry of the cyclic oligomers.

The racemization of an enantiopure sample of **4d** proceeded slowly at 70 °C in octane, and was completed after ca. 10 h. The rate of racemization was determined by classical kinetics to give rate constant $k = 3.5 \times 10^{-5}\,s^{-1}$, corresponding to $\Delta G^{\neq}_{343} = 114 \pm 1\,kJ\,mol^{-1}$. No racemization was observed for the sample of **4c** even though it was heated at 140 °C in decane where it significantly decomposed within a few hours. This observation indicates that the lower limit of the barrier to racemization is 146 kJ mol^{-1} for **4c**. As illustrated in Scheme 2, the enantiomerization takes place only by the rotation of (1,5)-A [or (1,5)-N*] moiety regardless of the rotation of (9,10)-A moiety. Therefore, these barriers are necessarily equal to the rotational barrier of the former rotor. We failed to resolve the enantiomers of **4b** by chiral HPLC because the rotation of (1,5)-N takes place much more rapidly than the laboratory time scale.

Evaluation of Rotational Barriers. The above kinetic measurements are summarized as follows: (a) (1,4)-P in **4a** rotates rapidly, (b) either (1,5)-N or (9,10)-A, or both, in **4b** rotate rapidly, (c) (1,5)-N* and (9,10)-A in **4c** rotate very slowly, and (d) (1,5)-A and (9,10)-A in **4d** rotate very slowly. The facile rotation of (1,4)-P moiety in **4a** is reasonably understood by the linear connection similarly found in rotors in molecular gyroscopes with 1,4-bis(substituted ethynyl)benzene structures.[3] As for the other compounds with crank arylene moieties, their rotational barriers are enhanced in the order of **4b** $\ll$ **4d** $<$ **4c**. In the transition state of the rotation, one flanking side of the crank moiety should rotate into the macrocyclic ring to markedly increase steric interactions with (9,10)-A moiety. Hence, the transition state is greatly destabilized by the *t*-butyl groups in **4c** or the long crank moiety in **4d** compared with **4b** to enhance the rotational barriers. For **4d**, the free energies of activation determined by classical kinetics and spin saturation transfer methods correspond to the barriers to rotation of (1,5)-A and (9,10)-A, respectively, as discussed in the independent processes in Scheme 2. The difference between the two values, 114 and 102 kJ mol^{-1}, is small but significant even though we consider the experimental errors and the entropy of activation term. Namely, (9,10)-A rotates 65 times faster than (1,5)-A at the same temperature, and the correlated rotation would be unlikely in the cyclic structure. As regards **4c**, we could estimate only the lower limits of the rotational barriers of both rotors, which were larger than those for the corresponding rotors in **4d**. This means that the bulky alkyl groups at the flanking positions in the crank moiety effectively lock the conformation of the parallel oriented arene moieties. On the other hand, the information is rather limited for the rotation of (9,10)-A rotors in **4a** and **4b**. A molecular model revealed to us that its rotation would be slower than those of (1,4)-P in **4a** and (1,5)-N in **4b**, because of steric interactions of the terminal benzo moieties in (9,10)-A during the rotation.

The successful resolution of the enantiomers of **4c** and **4d** is solely due to the restricted rotation of the arylene moiety about the acetylene axes in the ring structure, as shown in Scheme 2. The observed barrier is the highest for cyclic diarylethyne systems, the barriers of which were experimentally established. This feature is attributed to the arrangement of arylene units, in which the transition state of rotation is severely destabilized by the steric congestion of the crank moiety. These findings will be helpful to predict rates of similar dynamic processes in other cyclic systems, the conformation of which is supposed to be locked.[9,24b,32] Cyclic tetramers **4b**–**4d** offer an interesting pedaling motion that can be a key function in molecular machines. Further studies are in progress to control the mode and rates of the pedaling motion to design such complex structures as a tandem pedaling device.

Experimental

General. Melting points are uncorrected. NMR spectra were measured on a JEOL GSX-400 (^{1}H: 400 MHz, ^{13}C: 100 MHz) or a JEOL Lambda 500 (^{1}H: 500 MHz, ^{13}C: 125 MHz) spectrometer. High-resolution mass spectra were measured on a JEOL MStation-700 spectrometer by FAB. Elemental analyses were performed on a Perkin-Elmer 2400 series analyzer. UV spectra were measure on a Hitachi U-3000 spectrometer with a 10 mm cell. Optical rotations were measured on a JASCO DIP-1000 digital polarimeter with a 3.5$\phi \times$ 100 mm cell. CD spectra were measured on a JASCO J-820 polarimeter with a 10 mm cylindrical cell. Column chromatography was carried out with Merck Silica Gel 60 (70–230 mesh) or Fuji Silysia Chromatorex-NH (100–200 mesh). 1,4-Diiodobenzene was commercially available.

Trimer 7. A solution of **5** (2.25 g, 5.13 mmol)[10b] and **6** (1.10 g, 1.10 mmol)[16] in a mixture of triethylamine (120 mL) and THF (120 mL) was degassed by bubbling Ar gas for 15 min. To the solution were added [Pd(PPh$_3$)$_4$] (593 mg, 0.513 mmol) and CuI (98 mg, 0.51 mmol). After the solution was refluxed for 96 h, the solvents were removed by evaporation. The crude product was purified by chromatography on silica gel with hexane–chloroform (9:1–4:1) as eluent to give the desired product as a brown solid. An analytical sample was obtained by recrystallization from hexane–chloroform. Yield 1.96 g (73%); mp 232–234 °C; ^{1}H NMR (CDCl$_3$, 500 MHz): δ 0.46 (6H, septet, J = 7.7 Hz), 0.65 (36H, d, J = 7.3 Hz), 1.06 (6H, t, J = 7.7 Hz), 1.63 (4H, sextet, J = 7.0 Hz), 1.84 (4H, quintet, J = 7.4 Hz), 3.67 (4H, t, J = 8.2 Hz), 7.47 (2H, dd, J = 7.1, 9.0 Hz), 7.57–7.62 (6H, m), 7.76 (2H, d, J = 6.7 Hz), 8.02 (2H, d, J = 6.4 Hz), 8.31 (2H, d, J = 9.2 Hz), 8.39 (2H, d, J = 8.9 Hz), 8.79 (4H, m), 9.67 (2H, s); ^{13}C NMR (CDCl$_3$, 125 MHz): δ 11.14, 14.12, 18.33, 23.42, 28.16, 33.78, 91.31, 97.04, 100.23, 104.91, 118.92, 122.50, 122.73, 123.21, 125.01, 125.04, 125.26, 125.76, 126.89, 127.58, 129.49, 131.00, 131.45, 131.50, 131.61, 132.50, 136.87 (1 aromatic signal missing); UV (CHCl$_3$): λ_{max} (ε) 265 (326000), 369 (16400), 389 (32300), 411 (43200), 442 nm (38500); FL (CHCl$_3$): λ_{max} 521 nm (λ_{ex} 393 nm), Φ_f 0.85; HRMS (FAB): calcd for $C_{76}H_{82}Si_2$ m/z 1050.5955, found m/z 1050.5955 [M$^+$]; Anal. Calcd for $C_{76}H_{82}Si_2$: C, 86.80; H, 7.86%. Found: C, 86.55; H, 7.78%.

Trimer 8. To a solution of **7** (200 mg, 0.190 mmol) in CH_2Cl_2 (38 mL) was added a 1.0 mol L^{-1} THF solution of TBAF (0.21 mL, 0.21 mmol). The solution was stirred at room temperature while checking the course of reaction by TLC. After 1.5 h, the reaction mixture was quenched with water (ca. 20 mL). The organic layer was separated, dried over $MgSO_4$, and evaporated. The residue was separated by chromatography on silica gel with hexane–chloroform (8:1) as eluent. Three compounds were eluted in the order of the starting material (**7**, 46%), **8**, and fully desilylated product (**9**, 11%). The desired compound was obtained as a brown solid. Yield 81 mg (48%); mp 142–144 °C; ^{1}H NMR (CDCl$_3$, 500 MHz): δ 0.46 (3H, septet, J = 7.1 Hz), 0.62 (18H, d, J = 7.4 Hz), 1.06 (6H, t, J = 7.4 Hz), 1.63 (4H, sextet, J = 7.4 Hz), 1.83 (4H, quintet, J = 7.4 Hz), 3.38 (1H, s), 3.64–3.68 (4H, m), 7.46–7.53 (2H, m), 7.59–7.65 (4H, m), 7.70–7.77 (3H, m), 7.83 (1H, d, J = 6.8 Hz), 8.03 (1H, d, J = 6.7 Hz), 8.12 (1H, d, J = 6.8 Hz), 8.29–8.40 (4H, m), 8.82 (2H, d, J = 8.6 Hz), 9.03 (2H, d, J = 8.6 Hz), 9.67 (1H, s), 9.85 (1H, s); ^{13}C NMR (CDCl$_3$, 125 MHz): δ 11.05, 14.07, 18.26, 23.37, 23.38, 28.08, 33.79, 33.81, 82.16, 83.29, 91.12, 92.23, 97.00, 100.45, 101.10, 104.86, 118.82, 119.03, 121.22, 122.34, 122.64, 122.67, 122.97, 123.16, 124.91, 125.00, 125.03, 125.24, 125.74, 125.81, 125.91, 126.95, 126.98, 127.74, 127.76, 129.37, 129.44, 129.46, 129.54, 130.85, 130.92, 131.11, 131.38, 131.42, 131.48, 131.59, 131.70, 132.29, 132.56, 136.88, 137.08 (1 aromatic signal missing); HRMS (FAB): calcd for $C_{67}H_{62}Si$ m/z 894.4621, found m/z 894.4665 [M$^+$]; Anal. Calcd for $C_{67}H_{62}Si$: C, 89.88; H, 6.98%. Found: C, 89.70; H, 7.17%. **9**: red solid; Yield 16 mg (11%); mp 344–346 °C; ^{1}H NMR (CDCl$_3$, 500 MHz): δ 1.07 (6H, t, J = 7.4 Hz), 1.64 (4H, sextet, J = 7.0 Hz), 1.84 (4H, quintet, J = 8.3 Hz), 3.36 (2H, s), 3.67 (4H, t, J = 8.3 Hz), 7.52 (2H, dd,

$J = 6.7$, 8.7 Hz), 7.64 (2H, dd, $J = 7.1$, 8.6 Hz), 7.75 (4H, m), 7.83 (2H, d, $J = 6.1$ Hz), 8.12 (2H, d, $J = 7.1$ Hz), 8.36 (2H, d, $J =$ 8.3 Hz), 8.39 (2H, d, $J = 8.2$ Hz), 9.04 (4H, m), 9.84 (2H, s); ^{13}C NMR ($CDCl_3$, 125 MHz): δ 14.04, 23.39, 28.12, 33.81, 82.23, 83.29, 92.30, 101.45, 118.97, 121.29, 122.62, 123.00, 124.95, 125.25, 125.81, 125.91, 127.02, 127.92, 129.44, 129.53, 130.82, 131.12, 131.47, 131.76, 132.40, 137.12; HRMS (FAB): calcd for $C_{58}H_{42}$ m/z 738.3287, found m/z 738.3278 [M^+]; Anal. Calcd for $C_{58}H_{42}$: C, 94.27; H, 5.73%. Found: C, 94.46; H, 5.80%.

Acyclic Tetramer 11a. A solution of **8** (76 mg, 0.085 mmol) and 1,4-diiodobenzene (**10a**) (140 mg, 0.425 mmol) in a mixture of triethylamine (40 mL) and THF (40 mL) was degassed by bubbling Ar gas for 15 min. To the solution were added [$Pd(PPh_3)_4$] (9.8 mg, 8.5 µmol) and CuI (1.6 mg, 8.5 µmol). After the solution was refluxed for 23 h, the solvents were removed by evaporation. The crude product was purified by chromatography on silica gel with hexane–chloroform (9:1) as eluent to recover 1,4-diiodobenzene and then with hexane–chloroform (4:1) as eluent to give the desired product as a brown solid. Yield 32 mg (34%); mp 226–227 °C; ^{1}H NMR ($CDCl_3$, 500 MHz): δ 0.45 (3H, septet, $J = 7.0$ Hz), 0.62 (18H, d, $J = 7.7$ Hz), 1.05–1.08 (6H, m), 1.59–1.68 (4H, m), 1.82–1.89 (4H, m), 3.66–3.70 (4H, m), 6.61 (2H, d, $J = 7.6$ Hz), 6.87 (2H, d, $J = 8.3$ Hz), 7.45–7.54 (6H, m), 7.60–7.65 (2H, m), 7.75 (1H, d, $J = 6.7$ Hz), 7.79 (1H, d, $J = 7.3$ Hz), 8.08 (1H, d, $J = 7.3$ Hz), 8.14 (1H, d, $J = 6.5$ Hz), 8.30 (1H, d, $J = 8.9$ Hz), 8.33 (1H, d, $J = 9.2$ Hz), 8.39 (2H, d, $J = 8.9$ Hz), 8.79–8.86 (4H, m), 9.68 (1H, s), 9.83 (1H, s); ^{13}C NMR ($CDCl_3$, 125 MHz): δ 11.09, 14.07, 18.28, 23.38, 23.39, 28.11, 28.13, 33.82, 33.86, 89.01, 91.30, 91.85, 93.97, 94.61, 97.05, 100.60, 100.73, 104.97, 118.32, 119.22, 122.15, 122.18, 122.49, 122.53, 122.77, 123.10, 123.23, 125.03, 125.05, 125.16, 125.19, 125.26, 125.54, 125.77, 125.83, 126.97, 127.13, 127.18, 127.65, 129.51, 129.52, 129.57, 129.60, 130.29, 130.57, 131.18, 131.45, 131.52, 131.56, 131.63, 132.38, 132.47, 132.52, 136.83, 136.88, 137.10 (1 aromatic signal missing); UV ($CHCl_3$): λ_{max} (ε) 269 (169000), 454 (33000), 474 nm (31000, sh); FL ($CHCl_3$): λ_{max} 524 nm (λ_{ex} 393 nm), Φ_f 0.52; HRMS (FAB): calcd for $C_{73}H_{65}ISi$ m/z 1096.3900, found m/z 1096.3864 [M^+]; Anal. Calcd for $C_{73}H_{65}ISi$: C, 79.90; H, 5.97%. Found: C, 79.83; H, 5.97%. A small amount of 1:2 coupling product **12a** was obtained as a brown solid: yield 15 mg (19%); mp 317–319 °C; ^{1}H NMR (500 MHz, $CDCl_3$): δ 0.41–0.50 (6H, m), 0.59 (36H, d, $J = 7.0$ Hz), 1.06–1.12 (12H, m), 1.59–1.69 (8H, m), 1.80–1.89 (8H, m), 3.62–3.71 (8H, m), 6.11 (4H, s), 7.02 (2H, dd, $J = 7.1$, 8.9 Hz), 7.20 (2H, dd, $J = 7.1$, 8.7 Hz), 7.34–7.41 (8H, m), 7.45 (2H, dd, $J = 7.0$, 8.9 Hz), 7.63 (2H, dd, $J = 6.7$, 9.3 Hz), 7.68 (2H, d, $J = 6.4$ Hz), 7.73 (2H, d, $J = 5.8$ Hz), 7.83 (2H, d, $J = 6.7$ Hz), 8.07 (2H, d, $J = 6.4$ Hz), 8.19 (2H, d, $J = 9.2$ Hz), 8.22 (2H, d, $J = 9.2$ Hz), 8.28 (2H, d, $J = 9.2$ Hz), 8.40 (2H, d, $J = 9.2$ Hz), 8.73 (4H, d, $J = 8.9$ Hz), 8.82 (4H, d, $J = 8.3$ Hz), 9.61 (2H, s), 9.82 (2H, s); HRMS (FAB) calcd for $C_{140}H_{126}Si_2$ m/z 1862.9398, found m/z 1862.9386 [M^+].

Acyclic Tetramer 11b. This compound was similarly prepared from **8** (101 mg, 0.113 mmol) and 1,5-diiodonaphthalene (**10b**)[33] (215 mg, 0.565 mmol). The crude product was purified by chromatography on silica gel with hexane–chloroform (4:1) as eluent to give the desired product as a brown solid. Yield 54 mg (42%); mp 237–239 °C; ^{1}H NMR ($CDCl_3$, 500 MHz): δ 0.33 (3H, septet, $J =$ 7.6 Hz), 0.53 (18H, d, $J = 7.0$ Hz), 1.04–1.09 (6H, m), 1.60–1.65 (4H, m), 1.82–1.87 (4H, m), 3.64–3.71 (4H, m), 6.49 (1H, t, $J =$ 7.7 Hz), 6.96 (1H, dd, $J = 7.4$, 8.7 Hz), 7.22 (1H, d, $J = 6.7$ Hz), 7.26–7.32 (2H, m), 7.35 (1H, d, $J = 7.3$ Hz), 7.45 (1H, dd, $J = 7.0$, 9.0 Hz), 7.57 (1H, dd, $J = 6.7$, 8.9 Hz), 7.62–7.67 (2H, m), 7.72 (1H, d, $J = 7.0$ Hz), 7.75 (1H, d, $J = 8.9$ Hz), 7.90 (1H, d, $J = 5.8$ Hz), 8.07 (1H, d, $J = 7.0$ Hz), 8.22 (1H, d, $J = 7.0$ Hz), 8.28 (1H, d, $J = 8.0$ Hz), 8.33 (1H, d, $J = 7.9$ Hz), 8.36 (1H, d, $J = 9.2$ Hz), 8.39 (2H, d, $J = 8.9$ Hz), 8.59 (2H, d, $J = 7.9$ Hz), 8.68 (2H, d, $J = 7.9$ Hz), 9.61 (1H, s), 10.11 (1H, s); ^{13}C NMR ($CDCl_3$, 125 MHz): δ 11.01, 14.08, 14.10, 18.21, 23.38, 23.41, 28.11, 28.13, 33.82, 33.88, 91.83, 92.44, 92.90, 93.07, 97.03, 100.36, 100.37, 104.89, 118.32, 118.95, 121.25, 122.48, 122.73, 122.76, 122.78, 123.23, 123.32, 125.00, 125.09, 125.23, 125.25, 125.28, 125.57, 125.68, 125.71, 126.19, 126.46, 126.56, 126.70, 126.78, 127.37, 129.49, 129.54, 129.64, 129.66, 130.19, 130.39, 130.71, 130.95, 131.40, 131.59, 131.62, 131.73, 131.78, 131.97, 132.05, 132.74, 133.19, 133.30, 136.84, 137.01, 137.20 (1 aromatic signal missing); UV ($CHCl_3$): λ_{max} (ε) 268 (153000), 476 nm (34000); FL ($CHCl_3$): λ_{max} 525 nm (λ_{ex} 393 nm), Φ_f 0.31; HRMS (FAB): calcd for $C_{77}H_{67}ISi$ m/z 1146.4057, found m/z 1146.4064 [M^+]. A small amount 1:2 coupling product **12b** was obtained as a yellow solid: yield 17 mg (16%); mp 336–337 °C; ^{1}H NMR ($CDCl_3$, 500 MHz): δ 0.28 (6H, septet, $J = 7.0$ Hz), 0.48 (36H, d, $J = 7.7$ Hz), 1.07 (6H, t, $J = 7.1$ Hz), 1.14 (6H, t, $J = 7.3$ Hz), 1.61 (4H, sextet, $J = 7.6$ Hz), 1.71 (4H, sextet, $J = 8.0$ Hz), 1.79 (4H, quintet, $J =$ 7.6 Hz), 1.92 (4H, quintet, $J = 7.6$ Hz), 3.61 (4H, t, $J = 8.0$ Hz), 3.75 (4H, t, $J = 7.9$ Hz), 6.29 (2H, dd, $J = 7.3$, 8.3 Hz), 6.49 (2H, d, $J = 6.7$ Hz), 6.82 (2H, dd, $J = 7.0$, 8.9 Hz), 7.14–7.21 (8H, m), 7.30 (2H, dd, $J = 6.7$, 9.2 Hz), 7.43 (2H, dd, $J = 6.7$, 9.0 Hz), 7.62–7.69 (6H, m), 7.77 (2H, d, $J = 7.0$ Hz), 7.95 (2H, d, $J =$ 8.9 Hz), 8.05 (2H, d, $J = 6.7$ Hz), 8.11 (2H, d, $J = 8.9$ Hz), 8.25–8.28 (4H, m), 8.44 (6H, d, $J = 9.2$ Hz), 8.59 (4H, d, $J = 8.0$ Hz), 9.48 (2H, s), 10.05 (2H, s); HRMS (FAB): calcd for $C_{144}H_{128}Si_2$ m/z 1912.9555, found m/z 1912.9555 [M^+].

Acyclic Tetramer 11c. This compound was similarly prepared from **8** (51 mg, 0.057 mmol) and 3,7-di-*t*-butyl-1,5-diiodonaphthalene (**10c**)[34] (141 mg, 0.286 mmol). The crude product was purified by chromatography on silica gel with hexane–chloroform (5:1) as eluent to give the desired product as a brown solid. Yield 31 mg (42%); mp 91–92 °C; ^{1}H NMR ($CDCl_3$, 500 MHz): δ 0.31 (3H, septet, $J = 6.7$ Hz), 0.50 (18H, d, $J = 7.7$ Hz), 1.03 (9H, s), 1.06–1.11 (6H, m), 1.25 (9H, s), 1.63–1.68 (4H, m), 1.78–1.94 (4H, m), 3.66–3.72 (4H, m), 7.12–7.18 (4H, m), 7.46 (1H, dd, $J = 7.0$, 9.0 Hz), 7.60–7.73 (7H, m), 7.95 (1H, d, $J = 6.8$ Hz), 8.09 (1H, d, $J = 6.8$ Hz), 8.18 (1H, d, $J = 7.1$ Hz), 8.24 (1H, d, $J = 1.3$ Hz), 8.30 (1H, d, $J = 9.2$ Hz), 8.39–8.42 (3H, m), 8.52–8.54 (2H, m), 8.61–8.63 (2H, m), 9.60 (1H, s), 10.10 (1H, s); ^{13}C NMR ($CDCl_3$, 125 MHz): δ 10.96, 14.08, 14.10, 18.15, 23.40, 23.40, 28.12, 28.20, 29.70, 30.78, 31.02, 33.82, 33.86, 34.45, 34.70, 91.66, 92.11, 92.63, 93.52, 97.03, 100.06, 100.35, 100.61, 104.79, 117.86, 118.71, 121.09, 121.89, 122.68, 122.73, 122.77, 122.80, 123.24, 125.00, 125.09, 125.21, 125.25, 125.45, 125.61, 126.34, 126.61, 127.24, 128.54, 129.47, 129.51, 129.60, 129.66, 130.28, 130.62, 130.96, 131.30, 131.49, 131.57, 131.73, 131.83, 131.94, 136.08, 136.79, 137.11, 148.37, 149.58 (8 aromatic signals missing); UV ($CHCl_3$): λ_{max} (ε) 269 (132000), 479 nm (32000); FL ($CHCl_3$): λ_{max} 525 nm (λ_{ex} 393 nm), Φ_f 0.41; HRMS (FAB): calcd for $C_{85}H_{83}ISi$ m/z 1258.5309, found m/z 1258.5284 [M^+]. A small amount of 1:2 coupling product **12c** was obtained as an orange solid: yield 13 mg (28%); mp 311–312 °C; ^{1}H NMR ($CDCl_3$, 500 MHz): δ 0.29 (6H, septet, $J = 7.7$ Hz), 0.48 (36H, d, $J = 7.3$ Hz), 0.88 (18H, s), 1.07 (6H, t, $J = 7.4$ Hz), 1.11 (6H, t, $J = 7.3$ Hz), 1.60–1.71 (8H, m), 1.80 (4H, quintet, $J = 7.3$ Hz), 1.90 (4H, quintet, $J = 7.7$ Hz), 3.62–3.65 (4H, m), 3.72 (4H, t, $J = 7.7$ Hz), 7.06–7.13 (8H, m), 7.16 (2H, dd, $J = 6.7$, 9.2 Hz), 7.22 (2H, d, $J = 1.9$ Hz), 7.31 (2H, dd, $J = 6.7$, 9.0 Hz), 7.43 (2H, dd, $J = 6.7$,

8.9 Hz), 7.64 (2H, dd, $J = 6.8$, 9.0 Hz), 7.69 (2H, d, $J = 6.7$ Hz), 7.80 (2H, d, $J = 6.4$ Hz), 7.90 (2H, d, $J = 6.7$ Hz), 8.07 (2H, d, $J = 6.4$ Hz), 8.10 (2H, d, $J = 1.9$ Hz), 8.23 (2H, d, $J = 8.9$ Hz), 8.26 (2H, d, $J = 8.0$ Hz), 8.28 (2H, d, $J = 8.6$ Hz), 8.41 (2H, d, $J = 9.2$ Hz), 8.46 (4H, d, $J = 8.3$ Hz), 8.63 (4H, d, $J = 8.6$ Hz), 9.53 (2H, s), 10.00 (2H, s); HRMS (FAB): calcd for $C_{152}H_{144}Si_2$ m/z 2025.0807, found m/z 2025.0802 [M^+].

Acyclic Tetramer 11d. This compound was similarly prepared from **8** (70 mg, 0.078 mmol) and 1,5-diiodoanthracene (**10d**)[35] (168 mg, 0.390 mmol). The crude product was purified by chromatography on silica gel with hexane–chloroform (5:1) as eluent to give the desired product as a brown solid. Yield 48 mg (51%); mp 124–144 °C (dec); ^{1}H NMR ($CDCl_3$, 500 MHz): δ 0.21 (3H, septet, $J = 7.6$ Hz), 0.45 (18H, d, $J = 7.6$ Hz), 1.06–1.11 (6H, m), 1.61–1.68 (4H, m), 1.81–1.91 (4H, m), 3.66–3.75 (4H, m), 6.46 (1H, t, $J = 7.6$ Hz), 7.11–7.19 (5H, m), 7.36 (1H, d, $J = 7.1$ Hz), 7.44 (1H, dd, $J = 7.4$, 9.0 Hz), 7.57–7.73 (6H, m), 7.77 (1H, d, $J = 8.6$ Hz), 7.96 (1H, d, $J = 6.8$ Hz), 8.09 (1H, d, $J = 6.4$ Hz), 8.12 (2H, s), 8.28 (1H, d, $J = 8.9$ Hz), 8.34–8.43 (5H, m), 8.47 (2H, d, $J = 8.6$ Hz), 8.79 (1H, s), 9.55 (1H, s), 10.33 (1H, s); ^{13}C NMR ($CDCl_3$, 125 MHz): δ 10.92, 14.08, 14.10, 18.10, 23.39, 23.42, 28.10, 28.18, 33.82, 33.91, 91.96, 92.67, 93.11, 93.83, 97.04, 98.80, 100.00, 100.13, 104.78, 117.72, 118.42, 120.79, 122.68, 122.75, 122.89, 122.97, 123.24, 123.34, 124.48, 124.98, 125.12, 125.19, 125.31, 125.33, 125.52, 125.53, 125.60, 125.65, 125.89, 126.04, 126.12, 126.63, 127.01, 129.10, 129.48, 129.55, 129.62, 129.73, 130.08, 130.35, 130.51, 130.76, 130.89, 130.96, 130.98, 131.06, 131.22, 131.33, 131.57, 131.64, 131.83, 131.94, 136.51, 136.78, 137.30 (3 aromatic signals missing); UV ($CHCl_3$): λ_{max} (ε) 261 (183000), 430 (35000), 448 (35000), 483 nm (34000); FL ($CHCl_3$): λ_{max} 529 nm (λ_{ex} 393 nm), Φ_f 0.16; HRMS (FAB): calcd for $C_{81}H_{69}ISi$ m/z 1196.4213, found m/z 1196.4188 [M^+]. A small amount of 1:2 coupling product **12d** was obtained as an orange solid: yield 13 mg (17%); mp 327–328 °C; ^{1}H NMR ($CDCl_3$, 500 MHz): δ 0.15 (6H, septet, $J = 7.4$ Hz), 0.38 (36H, d, $J = 7.3$ Hz), 1.07 (6H, t, $J = 7.4$ Hz), 1.18 (6H, t, $J = 7.0$ Hz), 1.62 (4H, sextet, $J = 7.7$ Hz), 1.73–1.81 (8H, m), 2.01 (4H, quintet, $J = 7.7$ Hz), 3.59 (4H, t, $J = 7.7$ Hz), 3.82 (4H, t, $J = 7.9$ Hz), 6.38 (2H, dd, $J = 7.3$, 8.1 Hz), 6.50 (2H, dd, $J = 6.7$, 9.1 Hz), 6.86 (2H, d, $J = 6.1$ Hz), 6.92 (4H, dd, $J = 7.0$, 8.4 Hz), 7.04 (4H, dd, $J = 6.7$, 8.4 Hz), 7.23–7.26 (2H, m), 7.37–7.41 (4H, m), 7.44 (2H, d, $J = 6.7$ Hz), 7.63 (2H, d, $J = 6.7$ Hz), 7.69 (2H, dd, $J = 6.7$, 8.9 Hz), 7.88 (2H, d, $J = 6.4$ Hz), 8.00 (2H, d, $J = 9.2$ Hz), 8.08–8.09 (6H, m), 8.22 (2H, d, $J = 9.8$ Hz), 8.29 (2H, s), 8.34 (2H, d, $J = 8.9$ Hz), 8.43 (4H, d, $J = 8.5$ Hz), 8.48 (2H, d, $J = 8.6$ Hz), 9.35 (2H, s), 10.30 (2H, s); HRMS (FAB): calcd for $C_{148}H_{130}Si_2$ m/z 1962.9711, found m/z 1962.9700 [M^+].

Cyclic Tetramer 4a. To a solution of **11a** (32 mg, 0.029 mmol) in THF (15 mL) was added a 1.0 mol L^{-1} THF solution of TBAF (0.029 mL, 0.029 mmol). This solution was stirred for 20 min at room temperature. After triethylamine (30 mL) and THF (15 mL) were added, the solution was degassed by bubbling Ar gas for 15 min. To the solution were added [$Pd(PPh_3)_4$] (10 mg, 8.7 µmol) and CuI (1.7 mg, 8.7 µmol). After the solution was refluxed for 17 h under Ar, the solvents were removed by evaporation. The crude product was purified by chromatography on silica gel (NH) with hexane–chloroform (9:1) as eluent to give the desired product as orange crystals. Yield 17 mg (72%); mp 330–331 °C; ^{1}H NMR ($CDCl_3$, 500 MHz): δ 1.08 (6H, t, $J = 7.6$ Hz), 1.67 (4H, sextet, $J = 7.4$ Hz), 1.86 (4H, quintet, $J = 7.3$ Hz), 3.70 (4H, t, $J = 8.6$ Hz), 6.78 (4H, s), 7.47–7.50 (4H, m), 7.55 (2H, dd, $J = 6.7$, 8.9 Hz), 7.65 (2H, dd, $J = 6.7$, 8.9 Hz), 7.82 (2H, d, $J = 6.4$ Hz), 8.09 (2H, d, $J = 6.4$ Hz), 8.35 (2H, d, $J = 9.2$ Hz), 8.42 (2H, d, $J = 8.9$ Hz), 8.88–8.90 (4H, m), 9.87 (2H, s); ^{13}C NMR ($CDCl_3$, 125 MHz): δ 14.10, 23.39, 28.15, 33.84, 89.27, 91.29, 95.08, 100.63, 118.47, 122.16, 122.26, 122.53, 123.04, 125.17, 125.21, 125.54, 125.92, 127.20, 127.34, 129.51, 129.53, 130.31, 130.41, 130.82, 131.50, 131.52, 132.43, 137.10; UV ($CHCl_3$): λ_{max} (ε) 272 (131000), 420 (16600), 446 (23600), 481 nm (15300, sh); FL ($CHCl_3$): λ_{max} 525 nm (λ_{ex} 393 nm), Φ_f 0.67, τ_f 3.2 ns; HRMS (FAB): calcd for $C_{64}H_{44}$ m/z 812.3443, found m/z 812.3423 [M^+]; Anal. Calcd for $C_{64}H_{44}$: C, 94.55; H, 5.45%. Found: C, 94.38; H, 5.68%.

Cyclic Tetramer 4b. This compound was similarly prepared from **11b** (51 mg, 0.044 mmol) as above. A reaction mixture was refluxed for 17 h. The crude product was purified by chromatography on silica gel (NH) with hexane–chloroform (9:1) as eluent followed by recrystallization from *m*-xylene to give the desired product as orange crystals. Yield 10 mg (25%); mp 341–342 °C; ^{1}H NMR (CD_2Cl_2, 400 MHz): δ 1.09 (6H, t, $J = 7.2$ Hz), 1.68 (4H, sextet, $J = 7.2$ Hz), 1.89 (4H, quintet, $J = 8.0$ Hz), 3.74 (4H, t, $J = 7.6$ Hz), 6.90 (2H, dd, $J = 7.4$, 7.6 Hz), 7.24–7.27 (4H, m), 7.31 (2H, d, $J = 8.0$ Hz), 7.63 (2H, dd, $J = 6.8$, 8.8 Hz), 7.68 (2H, dd, $J = 6.8$, 8.8 Hz), 7.92 (2H, d, $J = 6.8$ Hz), 8.08 (2H, d, $J = 6.8$ Hz), 8.28 (2H, d, $J = 8.0$ Hz), 8.44 (2H, d, $J = 9.6$ Hz), 8.47 (2H, d, $J = 9.2$ Hz), 8.60–8.63 (4H, m), 10.06 (2H, s); ^{13}C NMR ($CDCl_3$, 125 MHz): δ 14.01, 23.21, 28.04, 33.73, 92.25, 92.26, 93.37, 100.28, 118.22, 120.69, 122.51, 122.60, 123.47, 125.24, 125.28, 125.47, 125.79, 126.27, 126.29, 126.34, 126.89, 126.91, 126.94, 129.58, 129.77, 130.04, 131.70, 131.84, 131.94, 132.58, 137.03; UV ($CHCl_3$): λ_{max} (ε) 262 (95100), 382 (13900), 482 nm (25900); FL ($CHCl_3$): λ_{max} 525 nm (λ_{ex} 393 nm), Φ_f 0.69, τ_f 3.1 ns; HRMS (FAB): calcd for $C_{68}H_{46}$ m/z 862.3600, found m/z 862.3572 [M^+]; Anal. Calcd for $C_{68}H_{46}$: C, 94.63; H, 5.37%. Found: C, 94.42; H, 4.92%.

Cyclic Tetramer 4c. This compound was similarly prepared from **11c** (30 mg, 0.024 mmol) as above. A reaction mixture was refluxed for 17 h. The crude product was purified by chromatography on silica gel (NH) with hexane–chloroform (9:1) as eluent followed by recrystallization from hexane to give the desired product as orange crystals. Yield 9.0 mg (36%); mp 361–363 °C (dec); ^{1}H NMR ($C_2D_2Cl_4$, 500 MHz): δ 1.02–1.08 (24H, m), 1.62 (4H, sextet, $J = 7.3$ Hz), 1.86 (4H, quintet, $J = 7.4$ Hz), 3.68 (4H, t, $J = 6.8$ Hz), 7.02 (2H, m), 7.20 (2H, m), 7.56 (2H, d, $J = 2.1$ Hz), 7.59–7.65 (4H, m), 7.95 (2H, d, $J = 6.7$ Hz), 8.05 (2H, d, $J = 6.7$ Hz), 8.11 (2H, d, $J = 2.1$ Hz), 8.37 (2H, d, $J = 8.9$ Hz), 8.39 (2H, d, $J = 8.5$ Hz), 8.51 (2H, d, $J = 8.9$ Hz), 8.54 (2H, d, $J = 8.9$ Hz), 9.96 (2H, s); ^{13}C NMR ($CDCl_3$, 125 MHz): δ 14.12, 23.44, 28.15, 30.81, 33.87, 34.52, 91.31, 92.21, 93.67, 100.49, 117.98, 120.52, 122.16, 122.61, 122.68, 123.36, 125.23, 125.27, 125.38, 125.71, 126.00, 126.38, 126.50, 126.80, 129.39, 129.58, 129.60, 129.96, 130.23, 130.97, 131.59, 131.61, 131.89, 131.95, 137.02, 147.69; UV ($CHCl_3$): λ_{max} (ε) 259 (81300), 379 (11600), 489 nm (23300); FL ($CHCl_3$): λ_{max} 547 nm (λ_{ex} 393 nm), Φ_f 0.74, τ_f 3.1 ns; HRMS (FAB): calcd for $C_{76}H_{62}$ m/z 974.4851, found m/z 974.4840 [M^+].

Cyclic Tetramer 4d. This compound was similarly prepared from **11d** (48 mg, 0.040 mmol) as above. The reaction mixture was refluxed for 17 h. The crude product was purified by chromatography on silica gel (NH) with hexane–chloroform (9:1) as eluent followed by recrystallization from *m*-xylene–hexane to give the desired product as orange plates. Yield 11 mg (30%); mp 330–332 °C (dec); ^{1}H NMR (CD_2Cl_2, 400 MHz): δ 1.11 (6H, t, $J = 7.2$ Hz), 1.70 (4H, sextet, $J = 8.0$ Hz), 1.88–1.92 (4H, m), 3.78 (4H, t,

$J = 8.0$ Hz), 7.08 (2H, dd, $J = 7.2$, 8.4 Hz), 7.14–7.18 (2H, m), 7.26–7.30 (2H, m), 7.38 (2H, d, $J = 6.4$ Hz), 7.61–7.72 (6H, m), 7.91 (2H, d, $J = 6.8$ Hz), 8.04 (2H, d, $J = 6.4$ Hz), 8.23 (2H, d, $J = 8.0$ Hz), 8.46 (2H, d, $J = 8.8$ Hz), 8.50 (2H, d, $J = 9.2$ Hz), 8.63 (2H, d, $J = 8.0$ Hz), 8.72 (2H, s), 10.36 (2H, s); ^{13}C NMR ($CDCl_3$, 125 MHz, 50 °C): δ 14.08, 23.46, 28.19, 34.00, 92.45, 92.75, 94.00, 100.02, 117.87, 120.44, 122.92, 123.01, 123.82, 124.41, 125.10, 125.37, 125.42, 125.43, 125.72, 126.18, 126.56, 126.61, 126.83, 129.57, 129.76, 129.78, 129.81, 129.85, 129.95, 130.49, 130.84, 130.99, 131.59, 132.23, 132.27, 137.19; UV ($CHCl_3$): λ_{max} (ε) 260 (159000), 453 (36300), 477 nm (30600); FL ($CHCl_3$): λ_{max} 547 nm (λ_{ex} 393 nm), Φ_f 0.54, τ_f 6.8 ns; HRMS (FAB): calcd for $C_{72}H_{48}$ m/z 912.3756, found m/z 912.3744 [M^+].

X-ray Analysis. Single crystals of **4a**, (−)-**4c**, and (±)-**4d** used for the measurements were grown from solutions in toluene, hexane/chloroform, and hexane/*m*-xylene, respectively. Diffraction data of **4a** and (±)-**4d** were collected on a Rigaku RAXIS-IV imaging plate diffractometer and a Rigaku Saturn diffractometer, respectively, with Mo Kα radiation ($\lambda = 0.71070$ Å) to a maximum 2θ value of 55.0°, and those of (−)-**4c** were collected on a Rigaku RAXIS-RAPID diffractometer with Cu Kα radiation ($\lambda = 1.54187$ Å) to a maximum 2θ value of 136.4°. The reflection data were corrected for the Lorentz-polarization effects and secondary extinction. The structure was solved by the direct method (SHELX97)[36] and refined by the full-matrix least-squares method. Non-hydrogen atoms except some solvent atoms in (±)-**4d** were refined anisotropically. Hydrogen atoms were refined using the riding model. **4a**: crystal dimension 0.40 × 0.30 × 0.10 mm^3; formula $C_{64}H_{44}$, $M_r = 812.99$; monoclinic, space group $P2_1/n$ (No. 14), $a = 13.1251(2)$, $b = 12.1275(2)$, $c = 27.4773(3)$ Å, $\beta = 99.2810(6)°$, $V = 4316.43(11)$ Å^3, $Z = 4$, $D_{calcd} = 1.251$ g cm^{-1}, μ(Mo Kα) = 0.071 mm^{-1}, $T = 173$ K, $F(000) = 1712$, 9530 observed reflections, $R1 = 0.046$ [$I > 2.00\sigma(I)$], $Rw = 0.109$ (all data), GOF 1.04. (−)-**4c**: crystal dimension 0.19 × 0.18 × 0.16 mm^3; formula $C_{76}H_{62}$, $M_r = 975.33$; monoclinic, space group $P2_1$ (No. 4), $a = 10.06818(18)$, $b = 17.8794(3)$, $c = 15.8106(7)$ Å, $\beta = 105.3460(7)°$, $V = 2744.64(14)$ Å^3, $Z = 2$, $D_{calcd} = 1.180$ g cm^{-3}, μ(Cu Kα) = 5.011 cm^{-1}, $T = 93$ K, $F(000) = 1036$, 5185 observed reflections, $R1 = 0.0409$ [$I > 2.00\sigma(I)$], $wR2 = 0.1192$ (all data), GOF 1.11, Flack parameter 0.1(8).[37] (±)-**4d**: crystal dimension 0.31 × 0.08 × 0.06 mm^3; formula $C_{72}H_{48}\cdot 1/2(C_6H_{14})$, $M_r = 956.24$; triclinic, space group $P\bar{1}$ (No. 2), $a = 13.5511(19)$, $b = 14.798(2)$, $c = 14.896(3)$ Å, $\alpha = 106.893(6)°$, $\beta = 108.340(7)°$, $\gamma = 101.250(5)°$, $V = 2574.5(7)$ Å^3, $Z = 2$, $D_{calcd} = 1.289$ g cm^{-3}, μ(Mo Kα) = 0.726 cm^{-1}, $T = 93$ K, $F(000) = 1060$, 9822 observed reflections, $R1 = 0.084$ [$I > 2.00\sigma(I)$], $Rw = 0.244$ (all data), GOF 1.25. Crystallographic data have been deposited with the Cambridge Crystallographic Data Centre: Deposition numbers CCDC 748885 (**4a**), 748886 [(−)-**4c**], and 611249 [(±)-**4d**]. Copies of the data can be obtained free of charge via http://www.ccdc.cam.ac.uk/conts/retrieving.html (or from the Cambridge Crystallographic Data Centre, 12, Union Road, Cambridge, CB2 1EZ, U.K.; Fax: +44 1223 336033; e-mail: deposit@ccdc.cam.ac.uk).

Enantiomeric Resolution. Chiral HPLC was carried out with a Daicel CHIRALPAK® IA column (10 mmϕ × 250 mm) with hexane:2-propanol:chloroform 50:1:1 eluent. A solution of ca. 0.2 mg of (±)-**4d** in 2 mL of solvent was injected for each batch with flow rate of 1.0 mL min^{-1}. Enantiomers were eluted at 27.2 and 52.4 min with the separation factor α of 2.96. Easily eluted isomer: orange solid; mp 149–150 °C; $[\alpha]_D^{22}$ +800 (*c* 0.004, $CHCl_3$); CD ($CHCl_3$): λ ($\Delta\varepsilon$) 249 (−89.9), 272 (+227.7), 302 (+68.6), 360 (+23.3), 418 (−11.8). Less easily eluted isomer: orange solid; mp 150–152 °C; $[\alpha]_D^{22}$ −830 (*c* 0.004, $CHCl_3$); CD ($CHCl_3$): λ ($\Delta\varepsilon$) 250 (+84.7), 272 (−226.8), 302 (−71.9), 361 (−22.4), 416 (+12.5). Enantiomers of **4c** were similarly resolved with the same column with hexane:2-butanol 100:1 eluent. A solution of ca. 1.0 mg of (±)-**4c** in 5 mL of solvent was injected for each batch. Enantiomers were eluted at 33.2 and 34.4 min with the separation factor α of 1.07. Easily eluted isomer: orange needles, mp 334–335 °C (dec); $[\alpha]_D^{22}$ +800 (*c* 0.003, $CHCl_3$); CD ($CHCl_3$): λ ($\Delta\varepsilon$) 243 (−109.1), 284 (+55.8), 317 (−9.3), 359 (+13.6), 417 (−4.8). Less easily eluted isomer: orange needles, mp 340–342 °C (dec); $[\alpha]_D^{22}$ −850 (*c* 0.003, $CHCl_3$); CD ($CHCl_3$): λ ($\Delta\varepsilon$) 244 (+101.1), 284 (−53.8), 316 (+9.3), 361 (−12.7), 418 (+4.5).

Fluorescence Measurements. Fluorescence spectra were measured on a JASCO FP-6500 spectrofluorometer with a 10 mm cell at room temperature. The sample was dissolved in dichloromethane (1.0×10^{-5}–1.0×10^{-6} mol L^{-1}), which was degassed with Ar gas immediately before measurements. The spectra were measured upon excitation at 393 nm. The absolute fluorescence quantum yields were recorded on a Hamamatsu photonics C9920-02. The fluorescence lifetimes were measured on a Spectra-Physics time-resolved spectrofluorometer system (Tsunami 3960/50-M2S) with a Ti:Sapphire laser.

Kinetic Measurements. A sample of (−)-**4d** (2.5 mg) was dissolved in dry octane (5 mL). This solution was heated in a water bath at 70 ± 1 °C, and 0.5 mL of the solution was taken for analysis by chiral HPLC at appropriate intervals. The data were analyzed as reversible first-order equilibrium to afford the rate constant of racemization. Molar ratio of (−)-**4d** (time in s): 1.00 (0), 0.924 (1800), 0.888 (3600), 0.838 (5400), 0.795 (7200), 0.769 (9000), 0.730 (10800), 0.700 (14400), 0.643 (18000), 0.611 (21600). The least square fitting gave the following data: $k_{343} = (3.5 \pm 0.4) \times 10^{-5}$ s^{-1} and $\Delta G^{\neq}_{343} = 114 \pm 1$ kJ mol^{-1}. The experiments were carried out three times, giving comparable values. A sample of (−)-**4c** (2.0 mg) was dissolved in dry decane (6 mL), and heated at 140 °C. The sample was slightly decomposed without racemization, and completely decomposed after 11 h. The rate constant of racemization should be less than 3×10^{-6} s^{-1} (assuming <5% of racemization), and this value corresponds to $\Delta G^{\neq} > 146$ kJ mol^{-1}.

NMR Measurements for Kinetic Studies. VT ^{1}H NMR spectra were measured on the JEOL GSX-400 spectrometer. The temperature was read from a thermocouple after calibration with the chemical shift differences of signals of methanol or 1,2-ethanediol. The spectra at high temperature were measured in TCE-d_2, and those at low temperatures were measured in CD_2Cl_2 or $CDCl_3$. The saturation transfer experiments were performed on the JEOL Lambda-500 spectrometer, and the temperature was similarly calibrated as above. A sample of **4c** or **4d** was prepared by dissolving ca. 2 mg of sample in ca. 0.7 mL of TCE-d_2. After the 90° pulse width was determined in an ordinary manner, the effective spin lattice relaxation time (T_{1eff}/s) was measured by inversion-recovery. The rate of site exchange (k/s^{-1}) was calculated according to the following equation: $k = [(m/m_0)^{-1} - 1]/T_{1eff}$, where m and m_0 are signal intensities under and without irradiation, respectively. The intensity of the doublet at δ 8.16 was monitored under irradiation at the doublet at δ 8.56 for **4d**: $T_{1eff} = 2.2$ s, $m/m_0 = 0.63$, and $k = 0.27$ s^{-1} at 120 °C. The signal intensity of the triplet at δ 7.08 was not affected under irradiation of the triplet at δ 7.24 at 140 °C for **4c**: $T_{1eff} = 1.5$ s and $m/m_0 \approx 1$.

DFT Calculation. The calculations were carried out with Gaussian 03W[38] on a Windows computer. The structures of **4** were

optimized by hybrid DFT at the B3LYP/3-21G or M05/3-21G level. The input structures were generated from the X-ray structure or by preliminary optimization by AM1 calculation. The frequency analyses were carried out for the optimized structures to give no imaginary frequency. The calculations of excited states of **4c** and **4d** were calculated by TDDFT at the B3LYP/3-21G level to afford the excitation energies, oscillator strengths, transition velocity dipole moment, and transition magnetic dipole moments for the lowest 100 excited states. The CD spectra were obtained from these output data by a standard method reported previously.[30] Each excitation was treated as Gaussian function with half band width of 2000 cm^{-1}.

This work was partly supported by a Grant-in-Aid for Scientific Research on Priority Areas "Advanced Molecular Transformations of Carbon Resources" (No. 19020069) from MEXT (the Ministry of Education, Culture, Sports, Science and Technology) and by a matching fund subsidy for private universities from MEXT. The authors thank Professor T. Shinmyozu of Kyushu University for use of the X-ray diffractometer, Professor A. Orita and Associate Professor M. Takezaki of Okayama University of Science for assistance in fluorescence measurements, and Associate Professor K. Wakamatsu for helpful discussion in computational chemistry.

Supporting Information

MO charts and VT ^{1}H NMR of **4** and time-resolved fluorescence spectra of **4d**. This material is available free of charge on the web at http://www.csj.jp/journals/bcsj/.

References

1 Part of this work was preliminarily reported as a communication: T. Ishikawa, T. Shimasaki, H. Akashi, S. Toyota, *Org. Lett.* **2008**, *10*, 417; Part 14 of the series: S. Toyota, R. Azami, T. Iwanaga, D. Matsuo, A. Orita, J. Otera, *Bull. Chem. Soc. Jpn.* **2009**, *82*, 1287.

2 a) *Poly(arylene ethynylene)s*, ed. by C. Weder, Springer, Heidelberg, **2005**. b) T. M. Swager, in *Acetylene Chemistry*, ed. by F. Diederich, P. J. Stang, R. R. Tykwinski, Wiley-VCH, Weinheim, **2005**, Chap. 6. c) V. Balzani, M. Venturi, A. Credi, *Molecular Devices and Machines*, Wiley-VCH, Weinheim, **2003**. d) T. Kawase, *Synlett* **2007**, 2609. e) E. L. Spitler, C. A. Johnson, II, M. M. Haley, *Chem. Rev.* **2006**, *106*, 5344. f) W. Zhang, J. S. Moore, *Angew. Chem., Int. Ed.* **2006**, *45*, 4416.

3 a) S. D. Karlen, M. A. Garcia-Garibay, in *Topics in Current Chemistry: Molecular Machines*, ed. by T. R. Kelly, Springer, Berlin, **2005**, Vol. 262, p. 179. b) T.-A. V. Khuong, J. E. Nuñez, C. E. Godinez, M. A. Garcia-Garibay, *Acc. Chem. Res.* **2006**, *39*, 413. c) S. L. Gould, R. B. Rodriguez, M. A. Garcia-Garibay, *Tetrahedron* **2008**, *64*, 8336.

4 a) G. Vives, J. M. Tour, *Acc. Chem. Res.* **2009**, *42*, 473. b) Y. Shirai, J.-F. Morin, T. Sasaki, J. M. Guerrero, J. M. Tour, *Chem. Soc. Rev.* **2006**, *35*, 1043. c) J.-F. Morin, T. Sasaki, Y. Shirai, J. M. Guerrero, J. M. Tour, *J. Org. Chem.* **2007**, *72*, 9481. d) C. Joachim, H. Tang, F. Moresco, G. Rapenne, G. Meyer, *Nanotechnology* **2002**, *13*, 330. e) L. Grill, K.-H. Rieder, F. Moresco, G. Rapenne, S. Stojkovic, X. Bouju, C. Joachim, *Nat. Nanotechnol.* **2007**, *2*, 95.

5 a) K. Okuyama, T. Hasegawa, M. Ito, N. Mikami, *J. Phys. Chem.* **1984**, *88*, 1711. b) J. Seminario, A. G. Zacarias, J. M. Tour, *J. Am. Chem. Soc.* **1998**, *120*, 3970. c) Y. Li, J. Zhao, X. Yin, H. Liu, G. Yin, *Phys. Chem. Chem. Phys.* **2007**, *9*, 1186.

6 S. Toyota, T. Yanagihara, Y. Yoshida, M. Goichi, *Bull. Chem. Soc. Jpn.* **2005**, *78*, 1351.

7 O. Š. Miljanić, S. Han, D. Holmes, G. R. Schaller, K. P. C. Vollhardt, *Chem. Commun.* **2005**, 2606.

8 a) T. Makino, S. Toyota, *Bull. Chem. Soc. Jpn.* **2005**, *78*, 917. b) S. Toyota, T. Yamamori, T. Makino, *Tetrahedron* **2001**, *57*, 3521.

9 T. C. Bedard, J. S. Moore, *J. Am. Chem. Soc.* **1995**, *117*, 10662.

10 a) S. Toyota, M. Goichi, M. Kotani, *Angew. Chem., Int. Ed.* **2004**, *43*, 2248. b) S. Toyota, M. Goichi, M. Kotani, M. Takezaki, *Bull. Chem. Soc. Jpn.* **2005**, *78*, 2214.

11 S. Toyota, H. Miyahara, M. Goichi, S. Yamasaki, T. Iwanaga, *Bull. Chem. Soc. Jpn.* **2009**, *82*, 931.

12 S. Toyota, H. Miyahara, M. Goichi, K. Wakamatsu, T. Iwanaga, *Bull. Chem. Soc. Jpn.* **2008**, *81*, 1147.

13 S. Toyota, M. Kurokawa, M. Araki, K. Nakamura, T. Iwanaga, *Org. Lett.* **2007**, *9*, 3655.

14 Y. Tobe, M. Sonoda, in *Modern Cyclophane Chemistry*, ed. by R. Gleiter, H. Hopf, Wiley-VCH, Weinheim, **2004**, Chap. 1.

15 K. Campbell, R. R. Tykwinski, in *Carbon-Rich Compounds*, ed. by M. M. Haley, R. R. Tykwinski, Wiley-VCH, Weinheim, **2006**, Chap. 6.

16 B. F. Duerr, Y. S. Chung, A. W. Czarnik, *J. Org. Chem.* **1988**, *53*, 2120.

17 M. Nishio, M. Hirota, Y. Umezawa, *The CH/π Interactions: Significance in Molecular Recognition*, Wiley-VCH, New York, **1998**.

18 a) Y. Zhao, N. E. Schultz, D. G. Truhlar, *J. Chem. Theory Comput.* **2006**, *2*, 364. b) Y. Zhao, D. G. Truhlar, *J. Phys. Chem. A* **2006**, *110*, 10478. c) Y. Zhao, D. G. Truhlar, *Acc. Chem. Res.* **2008**, *41*, 157.

19 a) S. Akiyama, K. Nakasuji, M. Nakagawa, *Bull. Chem. Soc. Jpn.* **1971**, *44*, 2231. b) S. Akiyama, K. Nakashima, S. Nakatsuji, M. Nakagawa, *Dyes Pigm.* **1990**, *13*, 117.

20 L. Flamigni, A. M. Talarico, B. Ventura, R. Rein, N. Solladié, *Chem.—Eur. J.* **2006**, *12*, 701.

21 a) A. Iwama, T. Toyoda, M. Yoshida, T. Otsubo, Y. Sakata, S. Misumi, *Bull. Chem. Soc. Jpn.* **1978**, *51*, 2988. b) M. Morita, T. Kishi, M. Tanaka, J. Tanaka, J. Ferguson, Y. Sakata, S. Misumi, T. Hayashi, N. Mataga, *Bull. Chem. Soc. Jpn.* **1978**, *51*, 3449.

22 S. Nakatsuji, K. Matsuda, Y. Uesugi, K. Nakashima, S. Akiyama, W. Fabian, *J. Chem. Soc., Perkin Trans. 1* **1992**, 755.

23 I. Yamazaki, S. Akimoto, N. Aratani, A. Osuka, *Bull. Chem. Soc. Jpn.* **2004**, *77*, 1959.

24 a) P. Rademacher, in *Modern Cyclophane Chemistry*, ed. by R. Gleiter, H. Hopf, Wiley-VCH, Weinheim, **2004**, Chap. 11. b) M. Ohkita, K. Ando, T. Suzuki, T. Tsuji, *J. Org. Chem.* **2000**, *65*, 4385.

25 S. Toyota, S. Suzuki, M. Goichi, *Chem.—Eur. J.* **2006**, *12*, 2482.

26 a) R. L. Jarek, R. J. Flesher, S. K. Shin, *J. Chem. Educ.* **1997**, *74*, 978. b) J. Sandstrom, *Dynamic NMR Spectroscopy*, Academic, New York, **1982**.

27 T. Ikai, Y. Okamoto, *Chem. Rev.* **2009**, *109*, 6077.

28 S. Toyota, H. Onishi, K. Wakamatsu, T. Iwanaga, *Chem. Lett.* **2009**, *38*, 350.

29 a) V. Prelog, G. Helmchen, *Angew. Chem., Int. Ed. Engl.* **1982**, *21*, 567. b) E. L. Eliel, S. H. Wilen, *Stereochemistry of Organic Compounds*, Wiley, New York, **1994**, Chap. 14.

30 C. Diedrich, S. Grimme, *J. Phys. Chem. A* **2003**, *107*, 2524.
31 a) M. Parac, S. Grimme, *Chem. Phys.* **2003**, *292*, 11. b) S. Grimme, M. Parac, *ChemPhysChem* **2003**, *4*, 292.
32 M. A. Heuft, S. K. Collins, A. G. Fallis, *Org. Lett.* **2003**, *5*, 1911.
33 J. G. Rodríguez, J. L. Tejedor, *J. Org. Chem.* **2002**, *67*, 7631.
34 N. G. Pschirer, A. R. Marshall, C. Stanley, H. W. Beckham, U. H. F. Bunz, *Macromol. Rapid Commun.* **2000**, *21*, 493.
35 J. K. Kendall, H. Shechter, *J. Org. Chem.* **2001**, *66*, 6643.
36 G. M. Sheldrick, *Programs for Crystal Structure Determination from Single-Crystal Diffraction Data*, University of Göttingen, Germany, **1997**.
37 H. D. Flack, *Acta Crystallogr., Sect. A* **1983**, *39*, 876.
38 M. J. Frisch, G. W. Trucks, H. B. Schlegel, G. E. Scuseria, M. A. Robb, J. R. Cheeseman, J. A. Montgomery, Jr., T. Vreven, K. N. Kudin, J. C. Burant, J. M. Millam, S. S. Iyengar, J. Tomasi, V. Barone, B. Mennucci, M. Cossi, G. Scalmani, N. Rega, G. A. Petersson, H. Nakatsuji, M. Hada, M. Ehara, K. Toyota, R. Fukuda, J. Hasegawa, M. Ishida, T. Nakajima, Y. Honda, O. Kitao, H. Nakai, M. Klene, X. Li, J. E. Knox, H. P. Hratchian, J. B. Cross, V. Bakken, C. Adamo, J. Jaramillo, R. Gomperts, R. E. Stratmann, O. Yazyev, A. J. Austin, R. Cammi, C. Pomelli, J. W. Ochterski, P. Y. Ayala, K. Morokuma, G. A. Voth, P. Salvador, J. J. Dannenberg, V. G. Zakrzewski, S. Dapprich, A. D. Daniels, M. C. Strain, O. Farkas, D. K. Malick, A. D. Rabuck, K. Raghavachari, J. B. Foresman, J. V. Ortiz, Q. Cui, A. G. Baboul, S. Clifford, J. Cioslowski, B. B. Stefanov, G. Liu, A. Liashenko, P. Piskorz, I. Komaromi, R. L. Martin, D. J. Fox, T. Keith, M. A. Al-Laham, C. Y. Peng, A. Nanayakkara, M. Challacombe, P. M. W. Gill, B. Johnson, W. Chen, M. W. Wong, C. Gonzalez, J. A. Pople, *Gaussian 03, Revision E.01*, Gaussian, Inc., Wallingford CT, **2004**.